JOM, Vol. 64, No. 12, 2012
DOI: 10.1007/s11837-012-0474-2

Mechanistic-Based Lifetime Predictions for High-Temperature Alloys and Coatings

B.A. PINT,[1,4] S. DRYEPONDT,[1] A. ROUAIX-VANDE PUT,[2] and Y. ZHANG[3]

1.—Materials Science and Technology Division, Oak Ridge National Laboratory, Oak Ridge, TN 37830, USA. 2.—Institut Carnot CIRIMAT, ENSIACET, BP 44362, 31030 Toulouse Cedex 4, France. 3.—Department of Mechanical Engineering, Tennessee Technological University, Cookeville, TN 38505, USA. 4.—e-mail: pintba@ornl.gov

Increasing efficiency is a continuing goal for all forms of power generation from conventional fossil fuels to new renewable sources. However, increasing the process temperature to increase efficiency leads to faster degradation rates and more components with corrosion-limited lifetimes. At the highest temperatures, oxidation-resistant alumina-forming alloys and coatings are needed for maximum lifetimes. However, lifetime models accurate over the extended application durations are not currently available for a wide range of candidates and conditions. Increased mechanistic understanding and relevant long-term data sets will assist in model development and validation. Current progress is outlined for applying a reservoir-type model to Fe-base alloys and coatings. However, more work is needed to understand environmental effects, such as the presence of H_2O, and to extend the current model to NiCrAl and NiCr alloys. As the critical performance factors are better understood, it will be easier to evaluate new materials in laboratory screening experiments.

HIGHER TEMPERATURES: WHAT IS THE PROBLEM?

Increased efficiency is a continuing goal for propulsion or power generation whether it is fossil energy, nuclear power, or transportation because it lowers costs, fuel consumption, and specific emissions. The predominant strategy for increasing efficiency is higher process operating temperatures, leading to faster degradation rates and, in many cases, component lifetime limited by corrosion. At the same time that temperatures are increasing, the duty life required for components in these systems also is increasing; for example, 1,000,000 miles for heavy-duty diesel engines (~20000 h), 5-year (~40000 h) turbine overhaul schedules, or 30-year power plant lifetimes (~100000 h hot time for concentrated solar power).[1] Design and materials selection for these systems rely on accurate lifetime models to predict performance. While sometimes a quick calculation based on linear or parabolic reaction kinetics can provide guidance, often this approach is inadequate and/or there are limited data sets with the correct information on candidate alloys. Also, as the temperature increases, the number of candidate materials decreases rapidly. Iron-base alloys generally lose strength by 600°C for ferritic–martensitic steels and 700°C for austenitic steels.[1] Only a select group of alloys can operate for extended periods above 1000°C due to oxidation resistance limitations. Simply making parts thicker to accommodate the decrease in high-temperature strength or loss due to the environment is not realistic from the standpoint of cost, weight (especially in the case of transportation), and thermal fatigue. For example, the minimum 100-kh creep rupture life at 100 MPa criteria for boiler materials is based on experience with fatigue cracking of thick-walled tubing/piping.[2] Figure 1[3–5] gives an example of oxidation limitations at 1100°C comparing chromia-forming Haynes International alloy HR230 (Ni-27Cr-4W-0.004La, all compositions given in at.%) and alumina-forming oxide-dispersion-strengthened (ODS) alloy MA956 (Fe-20Cr-9Al-0.4Ti-0.2Y) formerly produced by Special Metals Corporation (Huntington, WV). As a function of specimen thickness, the 230 specimens showed a limited benefit of increasing specimen thickness (i.e., component wall thickness) on the time to where a dramatic increase in the total mass gain (specimen + spalled oxide) was observed, while the MA956 specimens

(Published online November 7, 2012)

showed a large increase in the time to breakaway oxidation (FeO_x formation) with increasing specimen thickness. For a heat exchanger with a 40-kh lifetime goal for a component at ~1100°C,[3] MA956 or another alumina-forming alloy appears to be a much better candidate.

Despite the relatively small number of candidates for the highest temperature applications, there are limited data available about their performance. Unlike mechanical properties where Larson–Miller plots can provide some indication of creep rupture lifetimes across a range of times and temperatures, there are no comparable parameters for high-temperature oxidation resistance. The alloy selection system for elevated temperatures (ASSET) database is very useful for conventional alloys, especially in mixed gas environments, but it has less data available over 1000°C and for alumina-forming alloys.[6] Even if a broader database existed, new applications often come with new requirements or new environments that can significantly affect performance. A seemingly simple change such as the addition of water vapor (found in all combustion environments) is still not fully understood in terms of its impact on materials performance at high temperatures.[5,7] With the increasing requirements and service parameters, it is simply not possible to investigate every material in every condition to the degree necessary. Thus, there is a growing need for accurate lifetime models to predict component lifetimes as a function of temperature, thickness, *etc*. Such models need to be based on fundamental mechanistic understanding (when available) of the degradation mechanisms and require long-term data for validation. Examples of progress are shown for (1) Fe-base alumina-forming alloys and coatings, (2) thin-walled austenitic steels, and (3) the effect of environment on lifetime. However, these results also make it clear that there is incomplete mechanistic understanding and critical data gaps for other groups of materials such as NiCrAl- and NiCr-based alloys.

LIFETIME MODELING: WHERE ARE WE NOW?

The reservoir model[8] for alumina-forming alloys equates Al consumption to form alumina and supply of Al in the following alloy:

$$Akt_b^n = d\rho(C_o - C_b) \quad (1)$$

where A is a constant, k is a rate constant, t_b is the time to breakaway, n = 0.5 for parabolic kinetics and 1 for linear kinetics, d is the specimen thickness, ρ is the alloy density, C_o is the starting Al content in the alloy, and C_b is the Al content where the material can no longer form a protective alumina scale and the metal is rapidly consumed by FeO_x formation, i.e., breakaway oxidation. For MA956, Fig. 1 illustrates that increasing specimen thickness (d) increased t_b, and from these results, the exponent n can be determined from Eq. 1. While n may be 0.5 or even 0.3 (cubic kinetics) for thin-walled FeCrAl foils with no scale spallation,[9] scale spallation dominates for thicker-walled components and $n \sim 1$.[10–12] The reservoir model assumes that (1) Al diffusion is sufficiently fast that Al gradients in the metal can be ignored and (2) the oxidation rate can be adequately captured by the constants k and n.[8] For chromia-forming alloys, Cr concentration gradients in the metal (especially austenitic alloys) generally have to be considered, making for a more complex analysis,[13,14] although a simplified approach has recently been proposed for thin-walled components.[15] However, the reservoir model may be applicable to ferritic Fe-Cr alloys where Cr diffusion is faster.[16]

Using time to breakaway (t_b) is convenient because it is an absolute comparison rather than more arbitrary assessments of scale spallation or mass change (Fig. 2b shows a portion of an MA956 coupon converted to FeO_x at breakaway). Measuring t_b can be used to assess the effect of temperature and cycle frequency (time between cooling to room temperature) on lifetime for an alloy like MA956 (Fig. 2a which includes the 1100°C results from Fig. 1). As expected, lower temperatures led to a significant increase in t_b. Increasing the number of thermal cycles (i.e., increasing the cycle frequency) at 1200°C increased scale spallation leading to faster consumption of the alloy Al reservoir and shorter lifetimes. For MA956, increasing the cycle frequency from 100 h to 1 h was equivalent to a 50°C temperature increase. For the concentrated solar power application, a new data set was added for 10-h cycles (Fig. 2a). Initially, 10-h cycles were assumed to lie between lifetimes for 1-h and 100-h cycles (dotted line). The actual failures were much

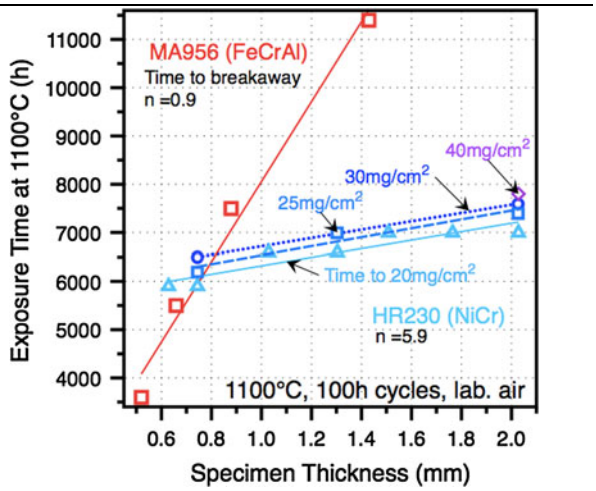

Fig. 1. Time to accelerated attack as a function of specimen thickness for NiCrW alloy 230 and ODS FeCrAl alloy MA956 for exposure in 100-h cycles at 1100°C in laboratory air. For MA956, the time is for the onset of Fe-rich oxide formation and increases significantly with thickness. For 230, the times are to total mass gains of 20–40 mg/cm^2. Values of n are given for Eq. 1. Adapted from Refs. 3 through 5.

closer than expected to the 100-h cycle lifetimes, especially for thinner specimens.

The data in Fig. 2a can be used to develop k as a function of temperature so that lifetimes can be predicted over a range of temperatures. However, the times required to generate data sets shown in Fig. 2a are still substantial, especially for more oxidation resistant alloys than MA956. Therefore, an additional methodology was developed based on Eq. 1. Figure 3a plots the change in alloy Al content as a function of exposure time starting with C_0 at $t = 0$ and the curve for each material ending at time t_b and Al content C_b. The exposure times were normalized for a 1.5 mm specimen thickness. These data for a number of Fe-base alumina-forming materials confirmed that the bulk Al content in the alloy dropped at a nearly linear rate when individual specimens were stopped and characterized by electron microprobe analysis (EPMA) at different times before breakaway at 1200°C in 1-h cycles.[12] This type of plot shows the value of C_b for wrought FeCrAlY (Fe-20Cr-10Al-0.08Y) as ~0 and for Fe-Al alloys as ~10%.[17] Recent data for dispersion-strengthened MA956 showed the same trend but with a C_b value of 1.7% Al for failure in dry O_2, similar to previously determined C_b values.[8,18–20] The slope of the line shows the rate at which Al is being consumed from the various alloys; MA956 has one of the faster rates due to scale spallation.

Based on the results in Fig. 3a, similar Al content studies performed at 1100°C with 100-h cycles in laboratory air could be used to predict longer lifetimes (Fig. 3b). Several specimens were exposed for 10–50 kh, but only the alloys with the lowest oxidation resistance reached failure. This type of plot clearly shows that MA956 lifetime was improved by the higher Al content in the MA956HT (Fe-22Cr-11Al-0.4Ti-0.2Y) alloy modification but did not reach the lifetime of Plansee ODS alloy PM2000 (Fe-20Cr-11Al-0.4Ti-0.2Y). Also, wrought FeCrAlY has a significantly longer lifetime than the ODS FeCrAl alloys because of less spallation and, therefore, a slower Al consumption. In comparison, the results for Fe_3Al-based alloys suggest its larger Al reservoir leads to much longer lifetimes at 1100°C, while the benefit of a high starting Al content was not as great at 1200°C. At 1200°C, Y-doped Fe-18Al showed a long lifetime by avoiding the high thermal expansion of the intermetallic Fe-Al phases and their higher scale spallation.[11] While publicly available data are still sparse for this type of work, by establishing the Al consumption rate at 1100°C and assuming a similar value of C_b as was determined at 1200°C,[17] lifetimes over 100 kh can be assumed for 1.5 mm thick FeCrAlY and iron aluminides.

For Al-rich coatings on Fe-base substrates, a similar reservoir type model can be used. However, in the case of a coating, the primary loss of Al is interdiffusion with the substrate so the rate of Al interdiffusion affects lifetime. There are several coating interdiffusion models available; see, for example, Refs. 21 and 22; however, diffusion data are lacking for most coating/alloy systems, as are the C_b values that define the end of life. For Al-rich coatings on ferritic–martensitic Grade 91 (Fe-9Cr-0.6Mo) steel, extensive work was performed on model coatings made by chemical vapor deposition to study diffusion rates at 500–800°C and determine C_b.[23,24] Predictions from the resulting lifetime model are shown in Fig. 4 for two different coating

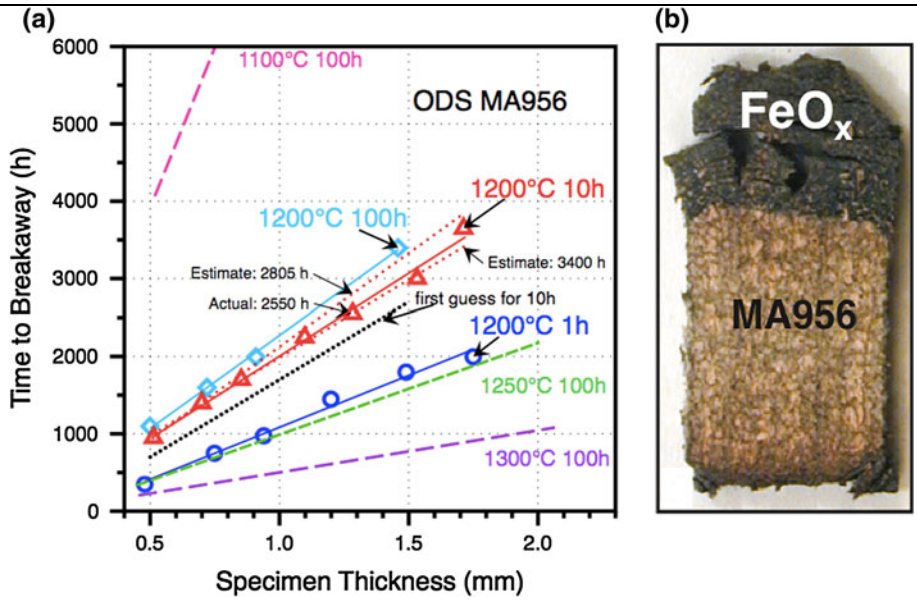

Fig. 2. (a) Time to breakaway oxidation (i.e., Fe-rich oxide formation) as a function of initial specimen thickness for ODS FeCrAl alloy MA956 under various cyclic conditions. Adapted from Refs. 4, 11, and 12. (b) 1.5 mm thick MA956 specimen cycled to breakaway oxidation after 1800 1-h cycles in dry O_2 at 1200°C, showing the thick Fe-rich oxide formation

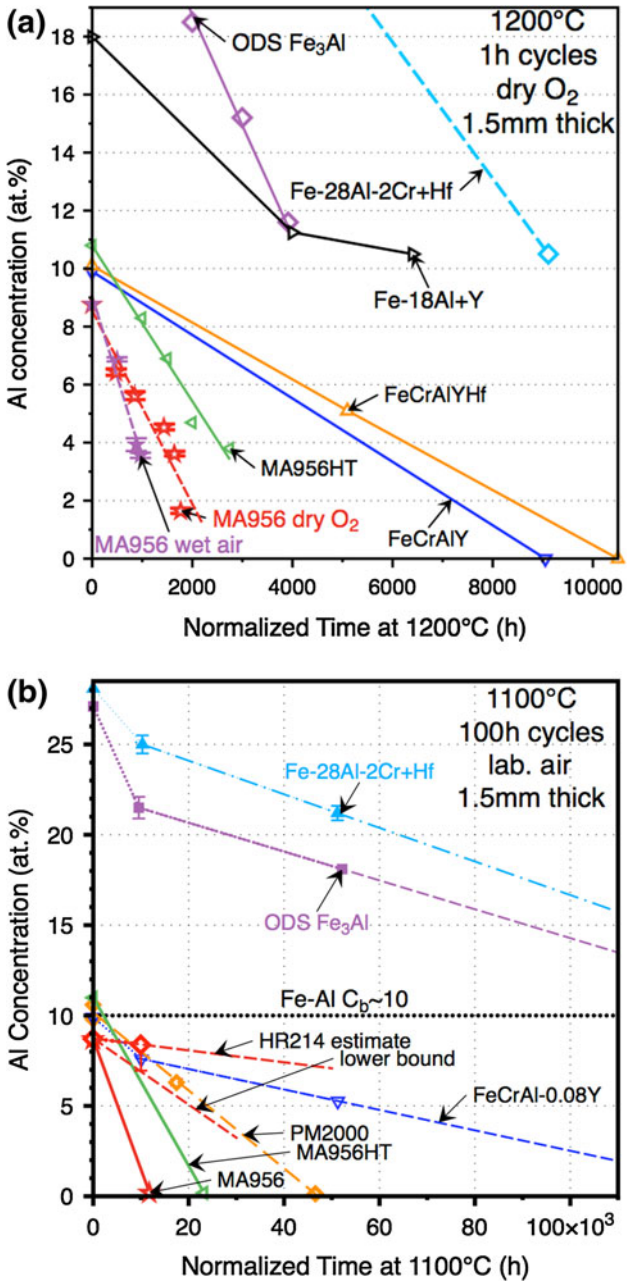

Fig. 3. Change in Al content as a function of normalized exposure time for various alumina-forming alloys (a) in 1-h cycles at 1200°C in dry O_2 and (b) in 100-h cycles at 1100°C in laboratory air. Adapted from Ref. 12.

thicknesses and two different exposure temperatures. The ~50-μm thick coatings had a starting surface Al content of ~18 at.%, while the 280-μm coatings had 26% Al at the surface. For sulfur-containing environments, C_b was assumed to be 20% Al[23] (Fig. 4); therefore, only the thicker coatings were applicable. However, the thinner coatings were protective in steam or wet air. For model development purposes, it was initially assumed that the surface Al content could not drop below ~8% Al, but failures at 700°C and 800°C showed the remaining Al content at the surface was ~3.4% at 700°C (star in Fig. 4) and <1% at 800°C. These temperatures are higher than application temperatures for Grade 91 but were needed to accelerate the degradation rate. No failures to determine C_b were obtained for exposures at 650°C up to 20 kh, and the thicker coatings were stopped after 20 kh at 700°C (noted in Fig. 4) when the predictions showed significantly longer lifetimes. The few available data points also have the error associated with variations in the starting coating thickness and Al content.

The coating failure shown in Fig. 4 was obtained by testing the coated specimen in air with 10% H_2O such that when the coating "failed," the steel

substrate was rapidly attacked by the environment. This "wet air" environment has been used as a surrogate for combustion gas in turbines and reciprocating engines where water vapor is present and detrimentally affects the oxidation behavior.[5,7] Alumina-forming alloys are generally thought to be resistant to the presence of water vapor due to the high thermodynamic stability of α-Al_2O_3 compared to other thermally grown oxides.[25] For alloys forming Cr_2O_3, the presence of water vapor and oxygen can result in greatly accelerated oxidation, especially for Fe-base alloys. Even for the most protective alloys, this environment results in the formation of volatile $CrO_2(OH)_2$ above ~600°C.[26,27] At long exposure times, the resulting paralinear kinetics associated with oxide growth and evaporation should lead to linear Cr loss rates, which are particularly significant for thin-walled heat exchangers (e.g., primary surface recuperators for small turbines) where the Cr reservoir is relatively small in a 80- to 100-μm thick foil.[28] While it has been possible to demonstrate linear Cr loss rates at 800°C in laboratory experiments, validating this mechanism at lower temperatures has been more difficult. Figure 5 shows the Cr loss from 90-μm HR120 (35Fe-35Ni-26Cr-0.4Nb) foil as a function of exposure time in dry and wet air and exhaust gas. The Cr loss is the average of three EPMA profiles across the foil. Both Cr depletion profiles and thickness loss need to be quantified. At 800°C, the addition of water vapor almost doubled the rate of Cr loss from the foil, and the specimen could not reach 10 kh exposure without accelerated attack, let alone the recuperator lifetime goal of 40 kh. However, at lower temperatures closer to the application temperature, the scatter in the data was significant at the longer exposure times, and there is still some question about applying linear kinetics for extremely long exposure times. An alumina-forming austenitic (AFA) steel (Fe-24Ni-15Cr-7Al-2Mn-1.5Nb-1Mo-0.3W) was developed for this application with sufficient creep strength for the recuperator application while retaining the enhanced oxidation resistance associated with an alumina scale.[29] Even after 10 kh exposure at 800°C in wet air, 100-μm AFA foil showed little degradation with an Al-rich oxide scale only a few micron thick.

While studies have been conducted on the water vapor effect on the growth and adhesion of alumina scales,[30–32] there were no data on its effect on t_b. Figure 6 shows the current status of an ongoing study[33] to evaluate t_b in different environments at 1200°C for MA956 and PM2000, which has significantly better oxidation resistance than MA956 (see also Fig. 3b). For both alloys, t_b dropped significantly for wet air compared to dry O_2. (To resolve the role of N_2 in air, a current group of MA956 specimens is running in dry air showing very similar lifetimes as dry O_2.) Clearly, there is a significant effect of adding water vapor, and the lifetimes predicted in Fig. 3b need to be reconsidered in light of these results. Surprisingly, a

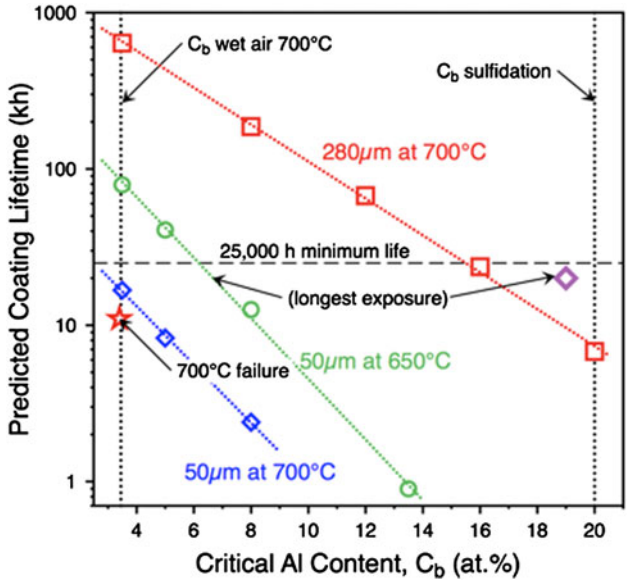

Fig. 4. Predicted coating lifetime as a function of the critical Al content on Gr.91 steels at coating failure for two different coating thicknesses and exposure temperatures. Experimental data points are shown as failure at 700°C (star) and surface coating content at 20 kh (diamond).

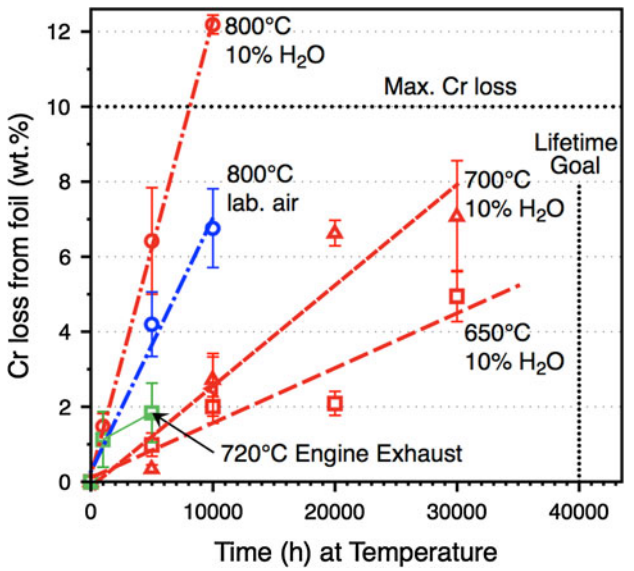

Fig. 5. Electron microprobe measured Cr loss from 80 to 90-μm foil specimens of alloy 120 exposed in laboratory air and wet air experiments at 650°C to 800°C and to microturbine exhaust at 720°C. A 40-kh lifetime is shown for reference. Adapted from Ref. 29.

combination of buffered CO_2 and H_2O (50%H_2O-50%(CO_2-0.15%O_2)) did not cause as large a drop in t_b as wet air (Fig. 6a). For PM2000, that experiment is still in progress with only the thinnest specimens failed (Fig. 6b). Initial work also is being conducted to understand if the drop in lifetime due to the presence of water vapor is caused by an increase in C_b or k.[33] Initial results in Fig. 3a for MA956 show no change in Al consumption after 500 h in wet air

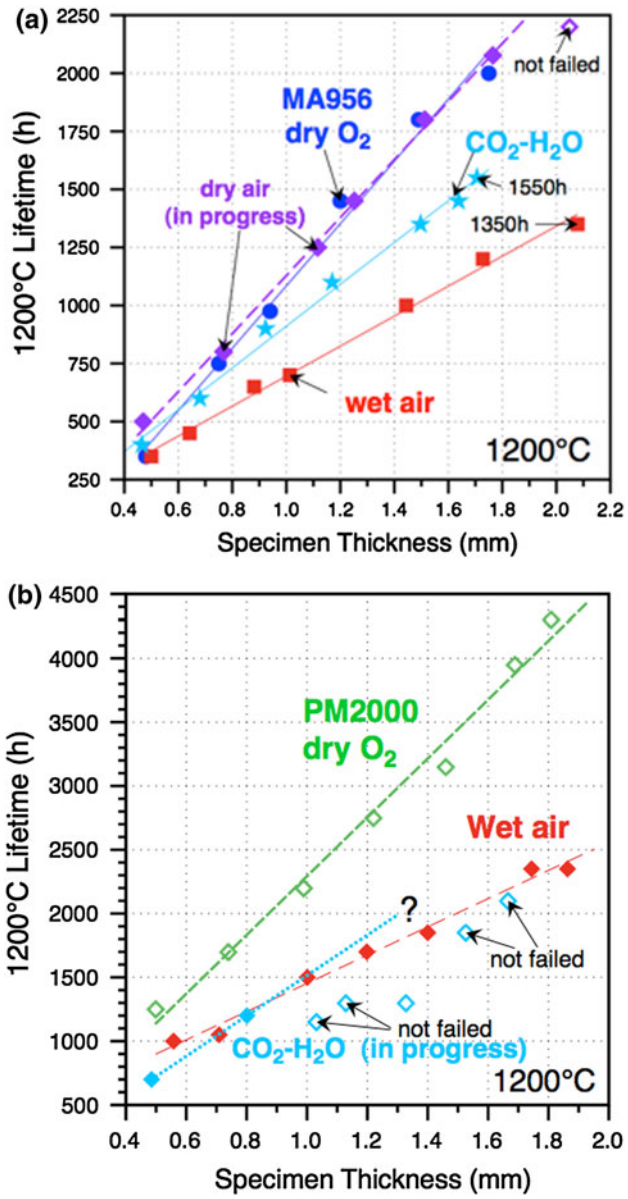

Fig. 6. Time to breakaway as a function of initial specimen thickness comparing dry O_2, dry air, air with 10% H_2O, and H_2O-50%(CO_2 + 0.15%O_2) for ODS FeCrAl alloys (a) MA956 and (b) PM2000. In all cases, the specimens are cooled in laboratory air. Adapted from Refs. 5 and 33.

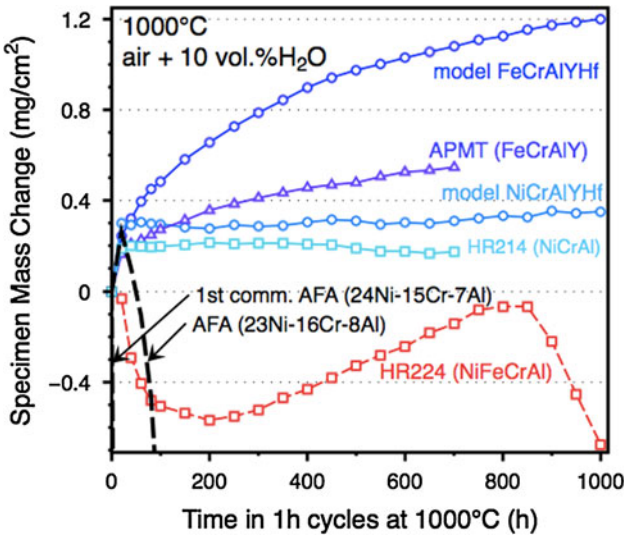

Fig. 7. Specimen mass change during 1-h cycles at 1000°C in wet air (10% H_2O) for several commercial and experimental alumina-forming alloys.

(suggesting no change in k) but a much higher C_b value at failure in water vapor.

For alloy development, one of the lessons learned from the environmental work is that, rather than collecting extensive data in laboratory air or dry O_2, a better starting point for screening of oxidation resistance is wet air. Figure 7 shows mass change data in 1-h cycles at 1000°C in wet air (10% H_2O). Two model MCrAlYHf (Fe/Ni-20Cr-9Al-0.03Hf-0.01Y) alloys showed comparable resistance to commercial alloys APMT (Fe-21Cr-10Al-2Mo-1Si-0.1Y-0.07Hf-0.06Zr) from Kanthal and NiCrAl alloy 214 (Ni-17Cr-9Al-3Fe) with low mass changes observed. In contrast, two new alloys, HR224 (Ni-28Fe-21Cr-7Al-0.4Ti) and Fe-based AFA, showed more spallation and, especially for AFA, rapid attack in these conditions. Even an increased Al (8.3%) level in AFA had a minimal effect at 1000°C.[34] Thus, AFA performance at 1000°C suggests it is limited to 900–950°C, and prior work on similar compositions in dry O_2 did not identify this limitation for austenitic alumina-forming steels.[35] It appears mixed Fe-Ni alloys (e.g., AFA and 224) do not perform as well as simpler FeCrAl or NiCrAl compositions, but the reason for this effect is not clear.

FUTURE WORK: WHAT IS NEEDED?

While frameworks have been suggested for predicting long-term oxidation resistance of alloys and coatings, the methodologies have not been thoroughly evaluated and tested. In many cases, attempting to predict lifetime revealed the limits of understanding. In Fig. 2, the 10-h cycles were conducted to simulate the concentrated solar power application, but the initial estimate (guess) of the effect on t_b relative to 100-h and 1-h cycles was not accurate. Furthermore, while it is attractive to only test thin specimens to minimize the experimental time, the dashed lines near the 10-h data set show lifetime predictions based on only the initial failures of the thinnest specimens in 10-h cycles. Of course, even thicker (>2 mm) specimens could further deviate from the predicted curve; thus, extrapolation of the current results is an issue. Gradients in Al do develop in thicker specimens,[17,33] which may reduce t_b, effectively making C_b dependent on thickness. A similar issue exists for coatings, where long coating lifetimes are desired for applications, but few

long-term exposures have been conducted to validate the coating oxidation and substrate interdiffusion model (COSIM)-based lifetime model (Fig. 4). A better understanding of the failure criteria, especially the effect of temperature and environment on C_b, will greatly increase confidence in the model predictions.

Another current limitation is that most of the data presented are for FeCrAl and Fe-Al alloys and coatings. However, Ni-base alloys are often more likely candidates for high-temperature applications because of their creep strength. Attempts to conduct similar studies on alloys like HR214 and the newer HR224 have met with problems. HR214 showed only a weak thickness effect at 1200°C,[4,17] and HR224 is not recommended for use above 1000°C and quickly showed large mass losses at 1200°C.[5] Initially, alloy 214 was included in the 1100°C lifetime study, and one data point is shown in Fig. 3b. Consistent with the low mass change, the bulk Al depletion was minimal after 10 kh exposure. However, the minimum surface Al content in the composition profiles was 6.9%, and using this value leads to a significantly lower lifetime prediction (Fig. 3b). Another issue is the lack of a C_b value for NiCrAl-type compositions. The only specimens taken to t_b at 1100°C were 60-μm foil, and the $C_b = 0$ in that case[17] is not likely to be relevant for thicker specimens. A similar situation exists for NiCr alloys. A different analysis is needed for the formation of Cr gradients (e.g., Ref. 15), but no mechanistic explanation has been developed yet for the results in Fig. 1. Perhaps at lower temperatures, a different thickness-failure relationship would be observed for NiCr alloys. The behavior of alloy 230 at 1100°C was similar to alloy 214 at 1200°C.[4,17]

Clearly, there is a great deal of work to be done before a comprehensive mechanistic model will be available to readily assist in design and materials selection for the next generation of high-temperature power generation systems. More progress will come as the current concepts are implemented in real-life predictions and mechanistic studies continue to improve our understanding of issues such as cycle frequency, multiple oxidants (CO_2, H_2O, *etc.*), and composition effects on high-temperature oxidation behavior.

ACKNOWLEDGEMENTS

Research was sponsored by the U. S. Department of Energy, Office of Fossil Energy, Advanced Research Materials Program and the Assistant Secretary for Energy Efficiency and Renewable Energy, Industrial Technologies Program (Combined Heat and Power). Ian Wright (retired, ORNL) helped initiate the ODS and Fe_3Al lifetime model studies. The authors are grateful to G. Garner (oxidation experiments) and L. Walker and D. Leonard (EPMA). P. Tortorelli and M. Brady provided useful comments on the manuscript.

REFERENCES

1. B.A. Pint, J.R. DiStefano, and I.G. Wright, *Mater. Sci. Eng.* 415, 255 (2006).
2. R. Viswanathan and W. Bakker, *J. Mater. Eng. Perform.* 10, 81 (2001).
3. B.A. Pint and J.R. Keiser, "Alloy Selection for High Temperature Heat Exchange" (Paper presented at NACE Corrosion 2006, San Diego, CA, 2006), NACE Paper 06-469.
4. B.A. Pint, *Shreir's Corrosion*, 4th ed., vol. 1. (Amsterdam: Elsevier, 2010), pp. 606–645.
5. B.A. Pint, *Mater. Sci. Forum* 696, 57 (2011).
6. R.C. John, A.D. Pelton, A.L. Young, W.T. Thompson, and I.G. Wright, *Mater. Sci. Forum* 461–464, 599 (2004).
7. W.J. Quadakkers, J. Żurek, and M. Hänsel, *JOM* 61 (7), 44 (2009).
8. W.J. Quadakkers and K. Bongartz, *Werkst. Korros.* 45, 232 (1994).
9. W.J. Quadakkers, D. Naumenko, E. Wessel, V. Kochubey, and L. Singheiser, *Oxid. Met.* 61, 17 (2004).
10. C.E. Lowell, C.A. Barrett, R.W. Palmer, J.V. Auping, and H.B. Probst, *Oxid. Met.* 36, 81 (1991).
11. B.A. Pint, W.D. Porter, and I.G. Wright, *Mater. Sci. Forum* 595–598, 1083 (2008).
12. B.A. Pint, L.R. Walker, and I.G. Wright, *Mater. High Temp.* 26, 211 (2009).
13. B. Gleeson and M.A. Harper, *Oxid. Met.* 49, 373 (1998).
14. H.E. Evans, A.T. Donaldson, and T.C. Gilmour, *Oxid. Met.* 52, 379 (1999).
15. D.J. Young, A. Chyrkin, and W.J. Quadakkers, *Oxid. Met.* 77, 253 (2012).
16. P. Huczkowski, N. Christiansen, V. Shemet, J. Piron-Abellan, L. Singheiser, and W.J. Quadakkers, *Mater. Corr.* 55, 825 (2004).
17. B.A. Pint, L.R. Walker, and I.G. Wright, *Mater. High Temp.* 21, 175 (2004).
18. J.P. Wilber, M.J. Bennett, and J.R. Nicholls, *Mater. High Temp.* 17, 125 (2000).
19. I. Gurrappa, S. Weinbruch, D. Naumenko, and W.J. Quadakkers, *Mater. Corr.* 51, 224 (2000).
20. H. Al-Badairy, G.J. Tatlock, and M.J. Bennett, *Mater. High Temp.* 17, 101 (2000).
21. R.W. Heckel, M. Yamada, C. Ouchi, and A.J. Hickl, *Thin Solid Films* 45, 367 (1977).
22. J.A. Nesbitt, *Lifetime Modelling of High Temperature Corrosion Processes*, ed. M. Schütze, W.J. Quadakkers, and J.R. Nicholls (London: Maney, 2001), pp. 359–378.
23. Y. Zhang, A.P. Liu, and B.A. Pint, *Mater. Corr.* 58, 751 (2007).
24. B.A. Pint and Y. Zhang, *Mater. Corr.* 62, 549 (2011).
25. E.J. Opila, *Mater. Sci. Forum* 461–464, 765 (2004).
26. H. Asteman, J.-E. Svensson, M. Norell, and L.-G. Johansson, *Oxid. Met.* 54, 11 (2000).
27. D.J. Young and B.A. Pint, *Oxid. Met.* 66, 137 (2006).
28. P.J. Maziasz, B.A. Pint, J.P. Shingledecker, N.D. Evans, Y. Yamamoto, K.L. More, and E. Lara-Curzio, *Int. J. Hydrogen Energy* 32, 3622 (2007).
29. B.A. Pint, M.P. Brady, Y. Yamamoto, M.L. Santella, P.J. Maziasz, and W.J. Matthews, *J. Eng. Gas Turbines Power* 133 (10), Article no. 102302 (2011).
30. C. Leyens, K. Fritscher, R. Gehrling, M. Peters, and W.A. Kaysser, *Surf. Coat. Technol.* 82, 133 (1996).
31. K. Onal, M.C. Maris-Sida, G.H. Meier, and F.S. Pettit, *Mater. High Temp.* 20, 327 (2003).
32. D.J. Young, D. Naumenko, E. Wessel, L. Singheiser, and W.J. Quadakkers, *Metall. Mater. Trans. A* 42, 1173 (2011).
33. A. Vande Put, S. Dryepondt, and B.A. Pint, "Cyclic Oxidation Behavior of ODS FeCrAl Alloys at High Temperature in H_2O and CO_2 Rich Atmospheres" (Paper presented at NACE Corrosion 2011, Houston, TX, 2011), NACE Paper 11-192.
34. M.P. Brady, K.A. Unocic, M.J. Lance, M.L. Santella, Y. Yamamoto, and L.R. Walker, *Oxid. Met.* 75, 337 (2011).
35. V. Ramakrishnan, J.A. McGurty, and N. Jayaraman, *Oxid. Met.* 30, 185 (1988).